Crystallization behaviour of Li$_2$O·Nb$_2$O$_5$·SiO$_2$ glass containing TiO$_2$ [#]

Srđan D. Matijašević[1], Vladimir D. Živanović[1], Mihajlo B.Tošić[1], Snežana R.Grujić[2],
Jovica N. Stojanović[1], Jelena D. Nikolić[1], Sonja V. Ždrale[2]

[1]*Institute for the Technology of Nuclear and other Mineral Raw Materials, 86 Franchet d' Esperey St, 11000 Belgrade, Serbia*
[2]*Faculty of Technology and Metallurgy, University of Belgrade, Karnegijeva 4, 11000 Belgrade, Serbia*

Abstract

This paper deals with the crystallization of glass 30Li$_2$O·15Nb$_2$O$_5$·50SiO$_2$·5TiO$_2$ (mol%). The crystallization behaviour was studied under isothermal and non-isothermal conditions. XRD and SEM methods were employed for determination of phase composition and microstructure of crystallized glass. It was detected that this glass crystallizes by the surface crystallization mechanism. SEM micrographs of the crystallized samples revealed that the crystals grow in the form of dendrites. The glass-ceramics with complex phase composition was obtained. Three crystalline phases were detected where LiNbO$_3$ has grown as primary phase and a secondary ones Li$_2$Si$_2$O$_5$ and SiO$_2$ appeared. The calculated average crystallite sizes are: 27 nm for LiNbO$_3$, 115 nm for Li$_2$Si$_2$O$_5$ and 45 nm for SiO$_2$. From the experimental data an activation energy of crystals growth, calculated using the Kissinger relation, is E$_a$ = 275 ±10 KJ / mol.

Keywords: lithium niobate, glass-ceramics, crystallization, crystal growth

I. Introduction

In the past few years very intensive investigations have been employed for the development of different ferroelectric materials for application in electronic and optoelectronic. Because of excellent optical, piezoelectric, photo-elastic, and photorefractive properties, lithium niobate crystals (LiNbO$_3$) are of great interest. Different glassy systems as SiO$_2$-Li$_2$O-Nb$_2$O$_5$, P$_2$O$_5$-Li$_2$O-Nb$_2$O$_5$ and B$_2$O$_3$-Li$_2$O-Nb$_2$O$_5$ have been studied to obtain glass-ceramics containing the LiNbO$_3$ ferroelectric phase [1–5]. Recently, the investigations are focused on the controlled crystallization of LiNbO$_3$-SiO$_2$-Al$_2$O$_3$ [6,7] or Bi$_4$Ti$_3$O$_{12}$-SiO$_2$ [8] glassy system and obtaining of transparent ferroelectric glass-ceramics. The transparency is possible to achieve with low and also with high crystallinity of glass-ceramics. The other specific properties of transparent glass-ceramics are connected directly with the characteristics of dominant crystalline phase. It was reported that the formation of ferroelectric LiNbO$_3$ crystallites in glass matrix is a complex process. The mechanism of crystallization includes the phase separation of glass, nucleation and growth of LiNbO$_3$ crystallites by nuclei coalescence in the clusters formed [6,7]. Regarding possible wide application of ferroelectric LiNbO$_3$ glass-ceramic the study of the crystallization of different glassy lithium niobate systems is very important. This work reports the results of crystallization of the glass 30Li$_2$O·15Nb$_2$O$_5$·50SiO$_2$·5TiO$_2$ (mol%). The investigation was performed under isothermal and non-isothermal crystallization conditions.

II. Experimental

The glass for experiments was prepared by the standard melt-quenching technique. Reagent grade Li$_2$CO$_3$, Nb$_2$O$_5$, SiO$_2$ and TiO$_2$ were mixed and homogenized in agate mortar and the mixture was melted in Pt-crucible in an electrical furnace (Carbolite, BLF 17/3) at T = 1450°C for t = 1 h. The melt was cast on a steel plate and cooled in air. The chemical analysis was performed using spectrophotometer (AAS Perkin Elmer Analyst 300). For the investigation under non-isothermal crystallization conditions one part of bulk glass sample was

crushed in agate mortar and then sieved to appropriate grain sizes. To determine crystallization mechanism for the DTA experiments the following glass granulations were chosen: < 0.048, 0.048–0.063, 0.063–0.1, 0.1–0.2, 0.2–0.3, 0.3–0.4, 0.4–0.5, 0.5–0.65, 0.65–0.83, 0.83–1 mm and 1–2 mm. The measurements were performed on a Netsch STA 409EP device by heating a constant sample mass of 100 mg at a rate of $\beta = 10°C/min$ in the temperature range $T = 25–1000°C$. The glass granulation < 0.048 mm was used for determination of kinetic parameters of crystallization and the DTA crystallization peaks were recorded at several heating rates, i.e., 5, 10, 12, 15 and 20°C/min. The glass transformation temperature (T_g), the temperature of crystallization peak (T_p) and liquidus temperature (T_l) of the glass were determined.

The experiments under isothermal condition were performed with bulk glass samples which were heated in the temperature range 650–830°C for different time from $t = 15$ min to $t = 100$ h. The XRD method was used to determine the phase composition of the crystallized glass. The XRD patterns were obtained on a Philips PW-1710 automated diffractometer using a Cu tube operated at 40 kV and 30 mA. The instrument was equipped with a diffracted beam curved graphite monochromator and a Xe-filled proportional counter. The diffraction data were collected in the 2θ Bragg angle ranging from 5 to 70°, counting for 1 s. A JEOL JSM 5800 SC microscope was used for the SEM investigations and the fractured bulk samples were previously sputtered with gold.

III. Results

X-ray powder diffraction (XRD) analysis confirmed the quenched melts to be amorphous. The solidified glass sample was transparent, light yellowish in colour and without residual bubbles.

The results of the chemical analyses of the glass are presented in Table 1. As shown in Table 1, the glass composition is close to the nominal one.

The DTA curve recorded for glass sample with grain size < 0.048 mm is presented in Fig. 1. As can be seen, the DTA curve recorded for glass sample with grain size < 0.048 mm shows the presence of one exothermal peak with maximum at $T_p = 723°C$ representing the glass crystallization and one endothermal indicating the melting of the crystals formed with liquidus temperature $T_l = 925°C$. The other significant temperatures, determined from DTA curve, are the glass transition temperature $T_g = 572°C$ and the crystallization onset temperature $T_x = 670°C$. The difference between the T_x-T_g ~98°C indicated that this glass is thermally stable.

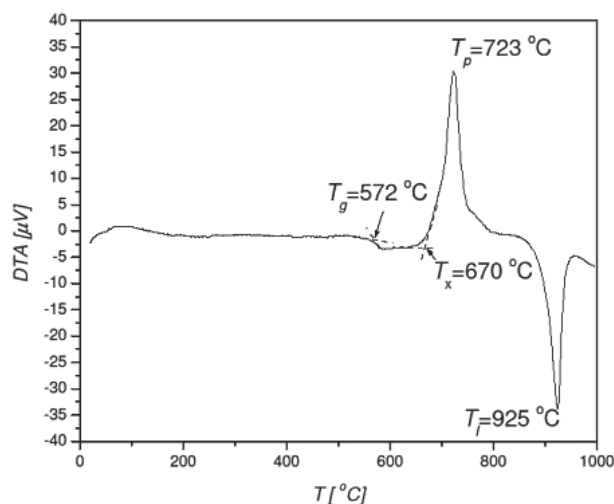**Figure 1. DTA curve of glass sample with grain size < 0.048 mm ($m = 100$ mg, $\beta = 10°C/min$)**

perature $T_x = 670°C$. The difference between the T_x-T_g ~98°C indicated that this glass is thermally stable.

To study the microstructure of isothermally treated bulk samples in the temperature rage of 650–830°C for different times the SEM method was employed and surface of crushed samples were recorded. In Fig. 2, SEM micrograph of glass sample heat treated at $T = 660°C$ for $t = 30$ min is shown. As shown in Fig. 2 the dendritic growth morphology of these crystals is present. Such morphology indicated the diffusion controlled crystal growth proceeding on crystal/glass interface.

In order to identify the formed crystal phases, experiments under isothermal conditions were performed with bulk samples. In a one-step regime, the samples were heated at $T = 650–830°C$ for different times. Figure 3 shows XRD pattern of glass sample thermally treated at $T = 830°C$ for $t = 100$ h. It can be seen that three crystalline phases appeared that clearly demonstrated a complex primary crystallization of this glass. The phase which was present in the largest amount crystallized as the primary one and the others appeared as secondary
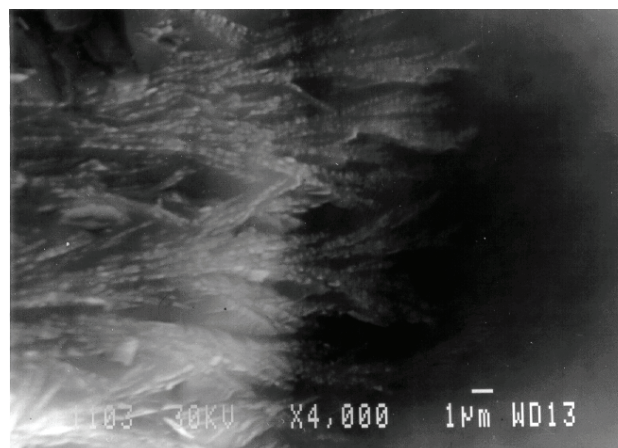
Table 1. Chemical analysis of the glass

| | Oxide content, x_i [mol%] | | | |
	SiO_2	Li_2O	Nb_2O_5	TiO_2
Nominal	50	30	15	5
Analyzed	51.22±0.5	29.64±1.0	15.14±0.5	4±0.5

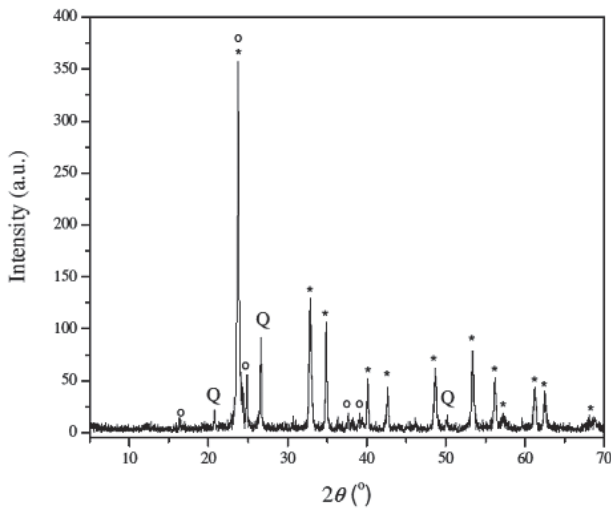**Figure 2. SEM micrograph of glass sample heat treated at $T = 660°C$ for $t = 30$ min**

Figure 3. XRD pattern of glass sample thermally treated at
$T = 830°$ **for** $t = 100$ **h. Peaks marked: *LiNbO₃**
JCPDS-74-2237, o-Li₂Si₂O₃ JCPDS-82-2396,
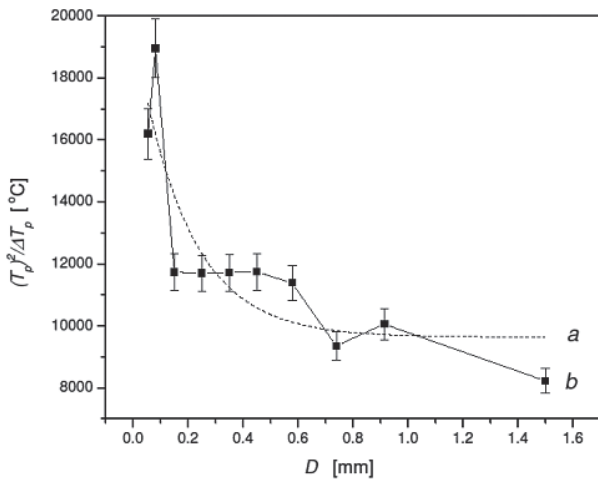**Q-SiO₂ JCPDS-46-1045 [9]**

Figure 4. $T_p^2 / (\Delta T)_p$ **as a function of glass particle size (D):**
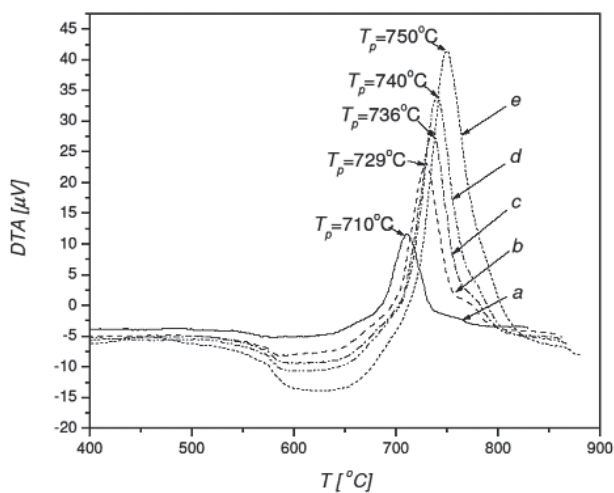***a*) theoretical curve *b*) experimental data**

Figure 5. DTA crystallization peaks T_p **recorded at heating**
rates: a) 5, b) 10, c) 12, d) 15 and e) 20°C/min
for the sample < 0.048 mm

phases. According to the results of XRD analysis, the crystallization of this glass commences by the formation of $LiNbO_3$ as the primary phase and $Li_2Si_2O_5$ and SiO_2 as secondary ones [9]. Crystallite domain size was calculated from X-ray powder diffraction data using Winfit 1.2 software on diffraction maximums (peaks) [10]. The average crystallite domain sizes are: 27 nm for $LiNbO_3$, 115 nm for $Li_2Si_2O_5$ and 45 nm for SiO_2.

IV. Discussion

The structure of this glass can be considered by using the structural random network model similar to vitreous silica. The three dimensional glass network is formed by linking of the corner-sharing SiO_4 tetrahedra and NbO_6 octahedra. As modifier cation Li^+ is located in vicinity of non-bridging oxygen of these network structural units (network holes) [11]. TiO_2 as a modifier oxide is present in small quantity in the glass and probably Ti ions are present in six-fold coordinated units in glass acting as a network modifier influencing the crystallization of glass.

For microstructure and properties of the crystallized samples, the knowing of the kinetic and crystallization mechanism of selected glass composition selected is crucial. To determine the dominant mechanism of glass crystallization a convenient method for DTA parameters evaluation proposed by Ray *et al.* [12] was used. Experimental and theoretical studies have shown that the particle size of glass powder influences the mechanism of its crystallization. The DTA crystallization peak parameters (δT_p) and $T_p^2 / (\Delta T)_p$ depend on specific mechanism of crystallization and are determined as a function of glass particle size (D). δT_p is the maximum of the peak height and is proportional to the total nuclei number present in the glass (surface and volume nuclei) [13]. The parameter $T_p^2 / (\Delta T)_p$ is related to the crystal growth dimension as follows [14]:

$$n = \frac{2.5 \cdot R}{Ea} \cdot \frac{T_p^2}{(\Delta T)_p} \qquad (1)$$

where R is the gas constant, E_a is the activation energy of crystal growth, $(\Delta T)_p$ is the width at half peak maximum and n is Avrami parameter. In Fig. 4 $T_p^2 / (\Delta T)_p$ as a function of glass particle size (D) is shown.

As may be seen in Fig. 4, the ratio $T_p^2 / (\Delta T)_p$ decreases by increasing the glass samples particle size that indicates a surface crystallization mechanism of glass. This is in accordance with previous theoretical prediction regarding the behaviour of parameters $T_p^2 / (\Delta T)_p$ and (δT_p). In the case of dominant surface crystallization mechanism the surface nuclei must dominate in glass sample. By increasing glass particle size the total effective surface area of the glass particles decreases and consequently the number of surface nuclei decreases, i.e. the total nuclei number decreases. This result was confirmed with SEM analysis of bulk heat treated glass

samples (Fig. 2). It was detected that crystals grow from the glass surface forming a crystal layer whit thickness increasing by increasing the annealing times.

For determination of the kinetic parameters of crystallization the glass sample granulation < 0.048 mm was chosen and the DTA crystallization peaks were recorded at several heating rates, i.e., 5, 10, 12, 15 and 20°C/min (Fig. 5).

For this case, the equation for the analysis of non-isothermal crystallization was derived by Matusita and Saka [15]:

$$\ln \frac{\beta^n}{T_p^2} = -\frac{m \cdot E_a}{R \cdot T_p} + const. \qquad (2)$$

where R is the gas constant. The values of the parameters n and m depend on the rate controlling mechanism of the crystallization kinetics, while the value of E_a is obtained from the ratio $\ln(\beta^n / T_p^2)$ versus $1/T_p$ using the corresponding values for n and m. Accordingly, to satisfy the condition of the constant number of nuclei during crystal growth, the glass powder with smallest particle size of < 0.048 mm was chosen. Since the crystal growth in these DTA experiments occurred on a constant number of nuclei, $n = m = 1$ (surface crystallization), equation (2) becomes the same as the well-known Kissinger equation [16]. In Fig. 6, the Kissinger plot $\ln(\beta^n / T_p^2)$ versus $1/T_p$ is presented and an activation energy of crystal growth was calculated from the slope of the line to be $E_a = 275 \pm 10$ KJ / mol.

In this case, Ozawa method [17] can also be applied for E_a calculation using the relationship:

$$\ln(\beta) = - (E_a / R\, T_p) + const. \qquad (3)$$

The activation energy $E_a = 291 \pm 10$ KJ/mol, calculated for crystal growth, is in a good agreement with Kissinger one.
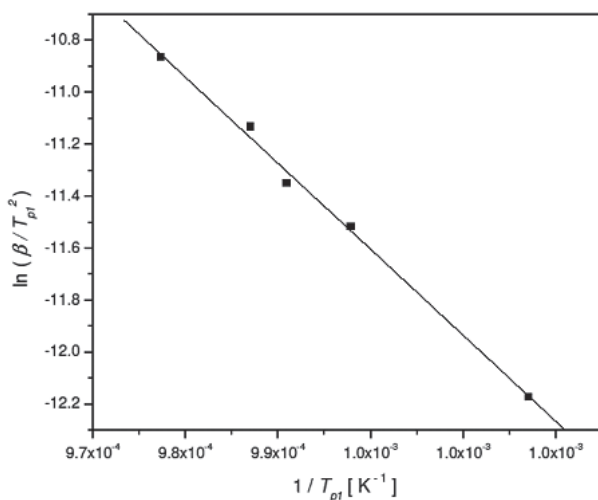

Figure 6. The Kissinger plot $\ln(\beta / T_p^2)$ vs. $1/T_p$ of glass sample < 0.048 mm

IV. Conclusions

The results of isothermal crystallization of the glass $30Li_2O \cdot 15Nb_2O_5 \cdot 50SiO_2 \cdot 5TiO_2$ (mol%) showed that a non-transparent white in colour glass-ceramics was obtained. The dominant surface crystallization mechanism with characteristic dendritic morphology of crystal growth was observed. For such morphology the diffusion controlled crystal growth proceeding on crystal/glass interface can be considered. The ferroelectric $LiNbO_3$ phase grows as primary one, while $Li_2Si_2O_5$ and SiO_2 appeared as secondary ones. For all three phases the crystallite domain size are presented in nanometers and the smallest one of the $LiNbO_3$ is 27 nm.

The values of activation energy for crystal growth calculated using the Kissinger and Ozawa relations are in good agreement.

References

1. G.E. Peterson, A.A. Ballman, P.V. Lenzo, M.P. Bridenbaugh, "Electro-optic properties of $LiNbO_3$", *Appl. Phys. Lett.*, **5** (1964) 62–64.
2. M.V. Shankar, K.B.R. Varma, "Dielectric and optical properties of surface crystallized TeO_2-$LiNbO_3$ glasses", *J. Non-Cryst. Solids*, **243** (1999) 192–203.
3. M.P.F. Graca, M.A. Valente, M.G. Perreira da Silva, "Electrical properties of lithium niobium silicate glasses", *J. Non-Cryst. Solids*, **325 (**2003) 267–274.
4. N. Syam Prasad, K.B.R. Varma, "Evolution of ferroelectric $LiNbO_3$ phase in a reactive glass matrix ($LiBO_2$-Nb_2O_5)", *J. Non-Cryst. Solids*, **351** (2005) 1455–1465.
5. E.B. De Araujo, J.A.C. De Paiva, A.S.B. Sombra, "The properties and crystallization of $LiNbO_3$ in lithium niobophosphate glasses", *J. Phys. Condens. Matter,* **7** (1995) 9723–9731.
6. Yi. Hu, C.L. Huang, "Crystallization kinetics of the $LiNbO_3$-SiO_2-Al_2O_3 glass", *J. Non-Cryst. Solids*, **278** (2000) 170–177.
7. Yi. Hu, C.L. Huang, "Crystal growth kinetics of $LiNbO_3$ crystals in Li_2O-Nb_2O_5-SiO_2-Al_2O_3 glass", *Mater. Res. Bull.*, **35** (2000) 1999–2008.
8. E.P. Kashchieva, M.Z. Krapchanska, S.S. Slavov, Y.B. Dimitriev, "Effect of synthesis route on the microstructure of SiO_2 doped bismuth titanate ceramics", *Process. Applic. Ceram.*, **3** [4] (2009) 171–175.
9. Joint Committee on Powder Diffraction Standards (JCPDS), Powder Diffraction Data, Cards No. 74-2237, 82-2396, 46-1045, Swarthmore, PA.
10. S. Krumm, Institut für Geologie, Schlossagartens, 91054 Erlangen, Germany
11. H.C. Zeng, K. Tanaka, K. Hirao, N. Soga, "Crystallization and glass formation in $50Li_2O \cdot 50Nb_2O$ and $25Li_2O \cdot 25Nb_2O_5 \cdot 50SiO_2$", *J. Non-Cryst. Solids*, **209** (1977) 112–121.

12. C.S. Ray, Q. Yang, W. Haung, D.E. Day, "Surface and internal crystallization in glasses as determined by differential thermal analysis", *J. Am. Ceram. Soc.*, **79** (1996) 3155–3160.
13. K.F. Kelton, K. Lakshmi Narayan, L.E. Levine, T.C. Cull, C.S. Ray, "Computer modeling of non-isothermal crystallization", *J. Non-Cryst. Solids*, **204** (1996) 13–31.
14. J.A. Augis, J.E. Bennett, "Calculation of the Avrami parameters for heterogenous solid-state reaction using a modification of the Kissinger method", *J. Thermal.*

Anal., **13** (1978) 283–292.
15. K. Matusita, S. Sakka, "Kinetic study on crystallization of glass by differential thermal analysis - Criterion on application of Kissinger plot", *J. Non-Cryst. Solids*, **38-39** (1980) 741–746.
16. H.E. Kissinger, "Reaction kinetics in differential thermal analysis", *Anal. Chem.*, **29** (1959) 1702–1706.
17. T. Ozawa, "A modified method for kinetic analysis of thermoanalytical data", *J. Thermal Analy.*, **9** (1976) 369–373.